JACS
JOURNAL OF THE AMERICAN CHEMICAL SOCIETY
Article
pubs.acs.org/JACS

Reversible and Irreversible Higher-Order Cycloaddition Reactions of Polyolefins with a Multiple-Bonded Heavier Group 13 Alkene Analogue: Contrasting the Behavior of Systems with $\pi-\pi$, $\pi-\pi^*$, and $\pi-n_+$ Frontier Molecular Orbital Symmetry

Christine A. Caputo,[†] Jing-Dong Guo,[‡] Shigeru Nagase,[‡] James C. Fettinger,[†] and Philip P. Power*[,†]

[†]Department of Chemistry, University of California, Davis, 1 Shields Avenue, Davis, California 95616, United States
[‡]Department of Theoretical and Computational Molecular Science, Institute for Molecular Science, Okazaki, Aichi 444-8585, Japan

Supporting Information

ABSTRACT: The heavier group 13 element alkene analogue, digallene $Ar^{iPr_4}GaGaAr^{iPr_4}$ (**1**) [Ar^{iPr_4} = C_6H_3-2,6-(C_6H_3-2,6-$^iPr_2$)$_2$], has been shown to react readily in [n + 2] (n = 6, 4, 2 + 2) cycloaddition reactions with norbornadiene and quadricyclane, 1,3,5,7-cyclooctatetraene, 1,3-cyclopentadiene, and 1,3,5-cycloheptatriene to afford the heavier element deltacyclane species $Ar^{iPr_4}Ga(C_7H_8)GaAr^{iPr_4}$ (**2**), pseudoinverse sandwiches $Ar^{iPr_4}Ga(C_8H_8)GaAr^{iPr_4}$ (**3**, **3^{iso}**), and polycyclic compounds $Ar^{iPr_4}Ga(C_5H_6)GaAr^{iPr_4}$ (**4**) and $Ar^{iPr_4}Ga(C_7H_8)GaAr^{iPr_4}$ (**5**, **5^{iso}**), respectively, under ambient conditions. These reactions are facile and may be contrasted with other all-carbon versions, which require transition-metal catalysis or forcing conditions (temperature, pressure), or with the reactions of the corresponding heavier group 14 species $Ar^{iPr_4}EEAr^{iPr_4}$ (E = Ge, Sn), which give very different product structures. We discuss several mechanistic possibilities, including radical- and non-radical-mediated cyclization pathways. These mechanisms are consistent with the improved energetic accessibility of the LUMO of the heavier group 13 element multiple bond in comparison with that of a simple alkene or alkyne. We show that the calculated frontier molecular orbitals (FMOs) of $Ar^{iPr_4}GaGaAr^{iPr_4}$ are of $\pi-\pi$ symmetry, allowing this molecule to engage in a wider range of reactions than permitted by the usual $\pi-\pi^*$ FMOs of C−C π bonds or the $\pi-n_+$ FMOs of heavier group 14 alkyne analogues.

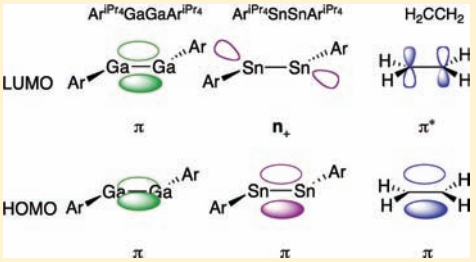

INTRODUCTION

The Diels−Alder [4π + 2π],[1] homo-Diels−Alder [2π + 2π + 2π],[2] and higher-order [6π + 2π] cyclizations[3] are of significant general and synthetic interest as they readily produce complex ring systems in a generally efficient manner.[4] Such polycycles are found in many natural products, but the synthetic organic cyclizations used to generate complex ring architectures generally require forcing conditions or the use of transition-metal catalysts.[5]

We showed recently that the reactions of heavier group 14 dimetallynes with cyclic polyolefins did not give the expected cyclization products. For example, the reactions of $Ar^{iPr_4}SnSnAr^{iPr_4}$ and $Ar^{iPr_4}GeGeAr^{iPr_4}$ [Ar^{iPr_4} = C_6H_3-2,6-(C_6H_3-2,6-$^iPr_2$)$_2$] with 1,3,5,7-cyclooctatetraene (COT) afforded the unique π-bound inverse-sandwich complexes [($Ar^{iPr_4}Sn$)$_2$(μ_2-η^2:η^3-COT)][6] and [($Ar^{iPr_4}Ge$)$_2$(μ_2-η^2:η^2-COT)],[7] respectively, the latter of which isomerized to a unprecedented tetracyclic cage digermane species (Scheme 1). Other cycloadditions with group 14 dimetallenes have been limited to reactions with 2π and 4π reaction partners, and no higher-order polyolefin cyclizations have been reported.

Very little is known, however, about the reactions of the neighboring heavier group 13 element analogues $Ar^{iPr_4}MMAr^{iPr_4}$ (M = Al, Ga, In, Tl) with polyolefins.[8] The digallene derivative, $Ar^{iPr_4}GaGaAr^{iPr_4}$ (**1**), has been shown to be reactive toward a variety of inorganic reagents.[9] It also reacts with 2,3-dimethyl-1,3-butadiene to form 1,6-digallacyclo-3,8-octadiene.[9] We recently showed that it reacts with the simple external olefins ethylene, propene, 1-hexene, and styrene to afford a series of compounds with 1,4-digallacyclohexane cores in which there is no Ga−Ga bonding.[10] However, under similar conditions, no reactions with internal olefins were observed.

We now show that the multiple-bonded group 13 heavy alkene analogue **1** reacts readily with norbornadiene (NBD) and quadricyclane, COT, 1,3-cyclopentadiene (CpH), and 1,3,5-cycloheptatriene (CHT) to afford the deltacyclane species

Scheme 1. Reactions of COT with $Ar^{iPr_4}EEAr^{iPr_4}$ (E = Sn,[6] Ge[7])

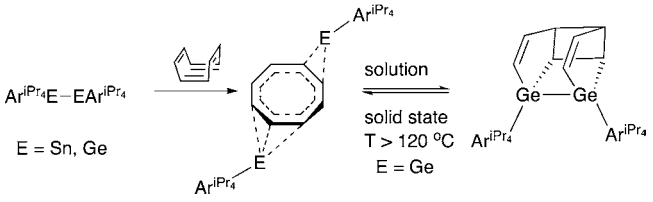

Received: February 15, 2012
Published: March 15, 2012

   dx.doi.org/10.1021/ja301247h | J. Am. Chem. Soc. 2012, 134, 7155−7164

Scheme 2. Cycloadditions of Various Polyolefins with $Ar^{iPr_4}GaGaAr^{iPr_4}$ (1)

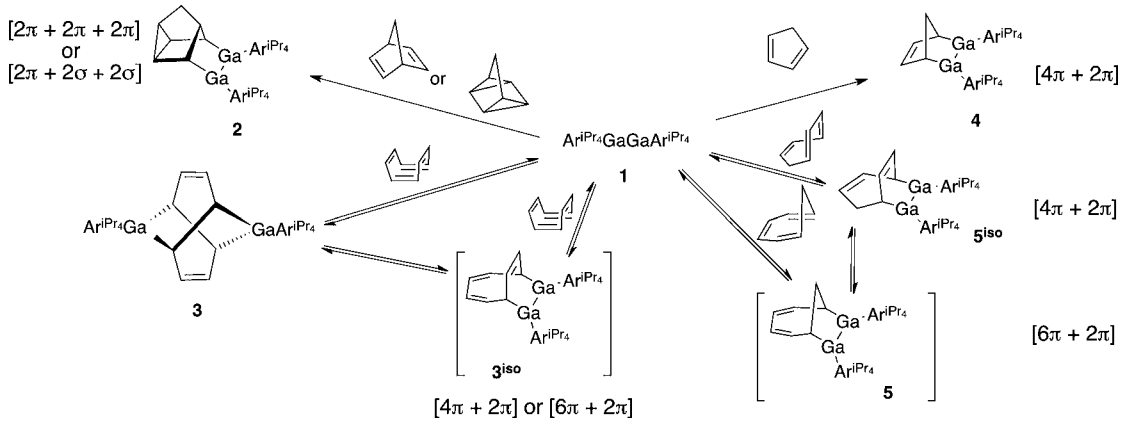

$Ar^{iPr_4}Ga(C_7H_8)GaAr^{iPr_4}$ (**2**) and the polycyclic compounds $Ar^{iPr_4}Ga(C_8H_8)GaAr^{iPr_4}$ (**3**, $\mathbf{3^{iso}}$), $Ar^{iPr_4}Ga(C_5H_6)GaAr^{iPr_4}$ (**4**), and $Ar^{iPr_4}Ga(C_7H_8)GaAr^{iPr_4}$ (**5**, $\mathbf{5^{iso}}$), respectively, under ambient conditions (Scheme 2). Unlike the heavier group 14 dimetallynes, the group 13 dimetallene reacts to afford cycloadducts that are in several instances analogous to the all-carbon versions. We show that they react much more readily than alkenes, without the need for substrate activation or the use of transition-metal catalysts. We propose that this effect is due to differences in the energy and symmetry of their frontier molecular orbitals (FMOs). In contrast to the all-carbon systems, the reactions are readily reversible. We show one example of onward isomerization of the cycloadduct that involves breaking of the Ga−Ga bond.

We have previously shown that in hydrocarbon solution, the dimetallene $Ar^{iPr_4}GaGaAr^{iPr_4}$ exists in equilibrium with the corresponding $Ar^{iPr_4}Ga$: monomers,[9,11] consistent with the dimetallene binding energy of ca. 9 kcal/mol calculated using density functional theory (DFT).[12] However, the reaction products described here all involve species that feature a Ga−Ga bond. The preservation of the Ga−Ga bond in the isolated products **2**, $\mathbf{3^{iso}}$, **4**, and $\mathbf{5^{iso}}$ suggests that the initial reaction involves the $Ar^{iPr_4}GaGaAr^{iPr_4}$ dimer and the cyclic polyolefin. In no case was a product with just a single gallium isolated. These observations tend to support the formulation of these heavier group 13 dimetallenes as multiply bonded $Ar^{iPr_4}GaGaAr^{iPr_4}$ dimers rather than as weakly associated $Ar^{iPr_4}Ga$: monomers.

EXPERIMENTAL SECTION

General Procedures. All manipulations were carried out under anaerobic and anhydrous conditions. All reagents were trap-to-trap vacuum-distilled and dried over 4 Å molecular sieves prior to use. **1** was prepared according to literature procedures.[9] ^{1}H, $^{13}C\{^1H\}$ correlation spectroscopy (COSY), and heteronuclear single-quantum correlation (HSQC) NMR spectra were recorded on Varian spectrometers and referenced to known standards.

$Ar^{iPr_4}Ga(C_7H_8)GaAr^{iPr_4}$ (2). To a solution of **1** (0.69 g, 0.073 mmol) in dry degassed hexane (50 mL) was added freshly distilled NBD (0.74 mL, 0.73 mmol) via syringe at ca. 25 °C. An immediate color change from dark-green to bright-orange was observed. The solution was stirred for 1 h, concentrated to ca. 10 mL under reduced pressure, and then stored at ca. −18 °C to afford orange crystals of **2**. Yield: 0.41 g, 56%. Mp: 207−210 °C. ^{1}H NMR (600 MHz, C_7D_8, 348 K): δ −0.26 (br d, GaC*H*, $^3J_{HH}$ = 4.8 Hz, 2H), 0.76 (s, $Ga(CHCH)_2CHCH_2$, 2H), 0.81 (s, GaCHC*H* and $Ga(CHCH)_2CHCH_2$, 2H), 0.85−0.89 (m, $Ga(CHCH)_2CHCH_2$, 2H), 0.98 (d, $CH(CH_3)_2$, $^3J_{HH}$ = 6.6 Hz, 12H), 1.02 (d, $CH(CH_3)_2$, $^3J_{HH}$ = 6.6 Hz, 12H), 2.90 (sept, $CH(CH_3)_2$, $^3J_{HH}$ = 6.6 Hz, 4H), 2.99 (sept, $CH(CH_3)_2$, $^3J_{HH}$ = 6.6 Hz, 4H), 6.84 (d, Ar, $^3J_{HH}$ = 7.8 Hz, 4H), 6.95 (m, Ar, 2H), 7.03−7.06 (m, Ar, 8H), 7.15 (t, $^3J_{HH}$ = 7.8 Hz, Ar, 4H). $^{13}C\{^1H\}$ NMR (C_6D_6, 100.6 MHz, 298 K): δ 11.3, 13.3, 23.7, 24.4, 25.2, 25.4, 30.8, 35.7, 36.3, 43.9, 122.9, 123.6, 126.2, 127.0, 128.4, 128.9, 129.3, 144.8, 156.5. IR (nujol mull) cm^{-1} (intensity): 2725 (m), 2670 (m), 2360 (m), 2340 (m). UV−vis λ_{max} (ε): 226 nm (3.3×10^4 M^{-1} cm^{-1}), 303 nm (8.6×10^3 M^{-1} cm^{-1}), 488 nm (2.4×10^3 M^{-1} cm^{-1}).

$Ar^{iPr_4}Ga(C_8H_8)GaAr^{iPr_4}$ (3). To a solution of **1** (0.30 g, 0.32 mmol) in dry degassed hexane (20 mL) was added freshly distilled COT (0.08 mL, 0.67 mmol) via syringe at ca. 25 °C. An immediate color change from dark-green to bright-yellow was observed. The solution was stirred for 1 h, concentrated to ca. 10 mL under reduced pressure, and then stored at ca. −18 °C to afford yellow crystals of **2**. Yield: 0.14 g, 42%. Mp: 170 °C (dec). Data for **3**: ^{1}H NMR (600 MHz, C_7D_8, 253 K): δ 1.04 (d, *o*-$CH(CH_3)_2$, $^3J_{HH}$ = 6.8 Hz, 24H), 1.13 (m, 4H), 1.24 (d, *o*-$CH(CH_3)_2$, $^3J_{HH}$ = 6.8 Hz, 24H), 2.42 (br, $Ga[CH(CHCH)CH]_2Ga$, 2H), 2.88 (sept, $CH(CH_3)_2$, $^3J_{HH}$ = 6.8 Hz, 8H), 4.00 (br, $Ga[CH(CHCH)CH]_2Ga$, 4H), 7.07 (m, Ar, 12H), 7.19 (m, Ar, 2H), 7.26 (m, Ar, 4H). $^{13}C\{^1H\}$ NMR (C_7D_8, 100.6 MHz, 273 K): δ 22.9, 23.2, 25.6, 25.9, 30.2, 30.7, 121.8, 123.3, 123.6, 127.6, 141.9, 146.6, 150.7. IR (KBr) cm^{-1} (intensity): 2964 (m), 2969 (m), 1942 (w), 1603 (w), 1464 (m), 1385 (m), 1363 (m), 1263 (s), 1099 (s), 1022 (s) 803 (s). UV−vis λ_{max} (ε): 416 nm (4.1×10^3 M^{-1} cm^{-1}), 330 nm (6.7×10^3 M^{-1} cm^{-1}), 242 nm (8.3×10^3 M^{-1} cm^{-1}). Data for $\mathbf{3^{iso}}$: ^{1}H NMR (800 MHz, C_7D_8, 313 K): δ 1.14−1.19 (m, $CH(CH_3)_2$, 18H), 1.25 (d, $CH(CH_3)_2$, $^3J_{HH}$ = 7.2 Hz, 6H), 2.97−3.01 (m, $CH(CH_3)_2$, 8H), 3.71 (q, $^3J_{HH}$ = 4.8 Hz, 1H), 4.27 (dd, $^3J_{HH}$ = 4.8 Hz, 1H), 4.58 (d, $^3J_{HH}$ = 12.8 Hz, 1H), 6.40 (dd, $^3J_{HH}$ = 12.8, 4.8 Hz, 1H), 7.16−7.32 (m, Ar, 18H). (For 2D HSQC and COSY spectra of a mixture of **3** and $\mathbf{3^{iso}}$, see Figures S5 and S6 in the Supporting Information.)

$Ar^{iPr_4}Ga(C_5H_6)GaAr^{iPr_4}$ (4). To a solution of **1** (0.21 g, 0.23 mmol) in dry degassed pentane (20 mL) was added freshly distilled CpH (0.15 mL, 1.4 mmol) via syringe at ca. 25 °C. An immediate color change from dark-green to dark-orange was observed. The solution was stirred for 1 h, concentrated to 5 mL under reduced pressure, and then stored at ca. −18 °C to afford orange crystals of **4**. Yield: 0.09 g, 40%. ^{1}H NMR (400 MHz, C_7D_8, 298 K): δ 0.95−1.08 (m, *o*-$CH(CH_3)_2$, 12H), 1.11−1.67 (m, *o*-$CH(CH_3)_2$, 12H), 1.20−1.31 (m, $(CHGa)_2$, CH*H*′$(CHGa)_2$, 2H), 2.71−3.12 (m, *o*-$CH(CH_3)_2$, C*H*H′$(CHGa)_2$, 9H), 5.89 (s, *H*C═C*H*, 2H), 7.08−7.31 (m, Ar, 18H). $^{13}C\{^1H\}$ NMR (C_6D_6, 150.6 MHz, 298 K): δ 13.9, 22.6, 24.0, 24.1, 25.5, 30.4, 30.5, 122.5, 123.1 (br), 126.7, 128.6 (br), 131.1, 140.7, 146.5, 146.7, 147.1. IR (neat) cm^{-1} (intensity): 3055 (w), 2958 (s), 2927 (m), 2866 (m), 1943 (w), 1651 (w), 1507 (m). UV−vis λ_{max} (ε): 264 nm (3.1×10^4 M^{-1} cm^{-1}), 351 nm (9.6×10^3 M^{-1} cm^{-1}), 435 nm (4.1×10^3 M^{-1} cm^{-1}).

$Ar^{iPr_4}Ga(C_7H_8)GaAr^{iPr_4}$ (5 and $\mathbf{5^{iso}}$). To a solution of $Ar^{iPr_4}GaGaAr^{iPr_4}$ (0.28 g, 0.30 mmol) in dry degassed pentane (20 mL) was added freshly distilled CHT (0.04 mL, 0.34 mmol) via

dx.doi.org/10.1021/ja301247h | J. Am. Chem. Soc. 2012, 134, 7155−7164

syringe at ca. 25 °C. An immediate color change from dark-green to dark-reddish-orange was observed. The solution was stirred for 1 h and concentrated to dryness under reduced pressure.

Data for **5**: Yield: 0.16 g, 54%. Mp: 122−124 °C (dec). ^{1}H NMR (600 MHz, C_7D_8, 298 K): δ 0.55 (br, *o*-CH(CH_3)$_2$, 12H), 0.87 (br, *o*-CH(CH_3)$_2$, 12H), 1.17 (br, *o*-CH(CH_3)$_2$, 12H), 1.25 (br, *o*-CH(CH_3)$_2$, 12H), 1.57 (d, $^2J_{HH}$ = 13.8 Hz, 1H), 2.31 (d, $^2J_{HH}$ = 16.8 Hz, 1H), 2.88 (br, *o*-CH(CH$_3$)$_2$, 4H), 2.94 (br, *o*-CH(CH$_3$)$_2$, 4H), 3.31 (br, 2H), 4.16 (br, 1H), 4.97 (br, 1H), 7.01 (br s, Ar, 4H), 7.02−7.12 (m, Ar, 10H), 7.22 (t, $^2J_{HH}$ = 7.8 Hz, Ar, 4H). ^{13}C{^{1}H} NMR (C_7D_8, 150.6 MHz, 298 K): δ 23.2, 25.3, 26.0, 30.1, 30.7, 31.4, 78.3, 98.9, 123.5, 126.8, 130.0, 141.8, 145.3, 146.7, 148.8, 155.2. UV−vis λ_{max} (ε): 440 nm (8.0×10^4 M^{-1} cm^{-1}), 350 nm (2.9×10^4 M^{-1} cm^{-1}), 262 nm (1.2×10^5 M^{-1} cm^{-1}).

After the NMR sample was heated to 373 K under nitrogen for 10 min, the solution changed from red to yellow. The yellow residue was taken up in a minimal amount of dry diethyl ether (ca. 5 mL) and then stored at ca. −18 °C to afford yellow crystals of **5**^{iso}.

Data for **5**^{iso}: Yield: 100% by ^{1}H NMR. Mp: 220−221 °C. ^{1}H NMR (600 MHz, C_7D_8, 373 K): −0.39 (dd, $^3J_{HH}$ = 9.0 Hz, $^2J_{HH}$ = 15.6 Hz, 1H), −0.25 (d, $^2J_{HH}$ = 15.6 Hz, 1H), 1.00−1.26 (m, 24H), 2.52 (t, $^3J_{HH}$ = 6.6 Hz, 1H), 2.74 (sept, *o*-CH(CH$_3$)$_2$, 4H), 2.83−2.95 (m, *o*-CH(CH$_3$)$_2$ and CH, 5H), 4.14 (pt, 1H), 4.78 (d, $^2J_{HH}$ = 13.2 Hz, 1H), 5.67 (dd, $^3J_{HH}$ = 6.6, Hz, $^2J_{HH}$ = 13.2 Hz, 1H), 5.77 (pt, 1H), 7.03−7.23 (m, Ar, 18H). ^{13}C{^{1}H} NMR (C_7D_8, 150.6 MHz, 298 K): δ 8.7, 23.3, 23.4, 30.6, 30.7, 30.7, 37.8, 52.1, 122.8, 123.1, 123.3, 123.4, 127.1, 131.6, 134.5, 138.9, 141.9, 142.2, 146.7, 146.8, 147.0, 147.1, 147.3, 150.4, 151.2. (See Figure S11 in the Supporting Information for the 2D COSY spectrum of a mixture of **5** and **5**^{iso}.)

RESULTS AND DISCUSSION

Reaction of 1 with Norbornadiene and Quadricyclane. The homo-Diels−Alder cycloaddition reactions of organic dienophiles with NBD and quadricyclane to furnish deltacyclanes has been well-documented experimentally and studied extensively by DFT analysis.[13] In general, the addition of an activated alkene to NBD proceeds via a $[2\pi + 2\pi + 2\pi]$ cyclization, which can be carried out either thermally[14] or in the presence of a transition-metal catalyst (Ni,[2,14] Cu,[15] Ru[16]) to give a homo-endo cyclization product. However, the addition of the same dienophiles to quadricyclane, a structural isomer of NBD, results in a $[2\pi + 2\sigma + 2\sigma]$ cyclization (Scheme 3) to give an exo-type product. The reactivity of NBD has previously been attributed to the dependence on a through-space interaction[17] and spatial proximity of the π bonds.[18] Both reactions can proceed either via a biradical stepwise mechanism or a concerted two-step mechanism.

Scheme 3. Reactions of NBD and Quadricyclane with Ar^{iPr_4}EEAr^{iPr_4} (E = Ga, Ge, Sn) and Other Dienophiles (R = H or Electron-Withdrawing Group, e.g., CN or COOR)

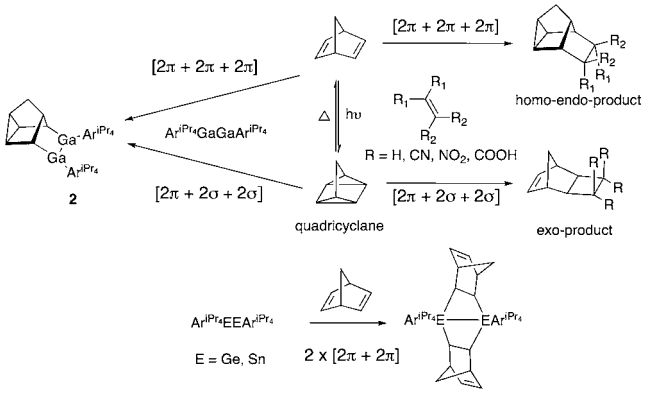

The above reactions differ greatly from the reactions of NBD with heavier group 14 alkyne analogues Ar^{iPr_4}EEAr^{iPr_4} (E = Ge, Sn), which react with 2 equiv of NBD to afford two reversible $[2\pi + 2\pi]$ reactions wherein the E−E σ bond is maintained (Scheme 3, bottom).[19] This behavior is in sharp contrast to the all-carbon alkyne reactivity, which exclusively undergoes $[2\pi + 2\pi + 2\pi]$ cycloaddition (via thermal and transition-metal-catalyzed routes).[20]

Our studies of the reaction of digallene with simple unactivated alkenes (ethylene, propene, 1-hexene, and styrene) revealed a double $[2\pi + 2\pi]$ cyclization in which the Ga−Ga bond is broken and 2 equiv of the alkene are added.[10] We attributed this reactivity to the in-phase interaction of the FMOs, namely, the highest occupied molecular orbital (HOMO) (in-plane π orbital) of the olefin and the lowest occupied molecular orbital (LUMO) (out-of-plane π orbital) of the digallene, which is symmetry-allowed.[12]

Addition of NBD to a solution of **1** in hexane results in an immediate color change from dark-green to bright-orange. Structural data revealed the formation of a polycyclic structure arising from a formal $[2\pi + 2\pi + 2\pi]$ cycloaddition reaction to furnish the homo-endo digalladeltacyclane product **2** (Figure 1). The Ga−Ga distance [2.4704(2) Å] lies at the longer end of

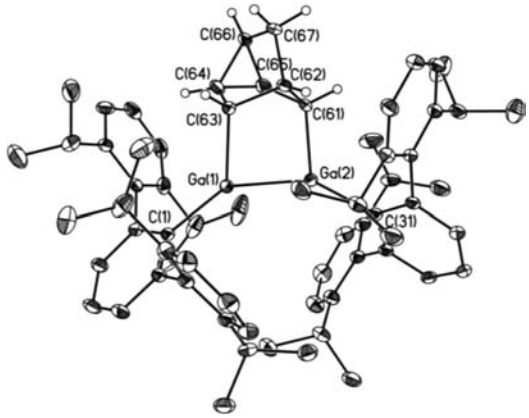

Figure 1. Thermal ellipsoid (30% probability) plot of **2**. Selected H atoms, a crystallographically independent deltacyclane molecule, and a cocrystallized hexane molecule are not shown. Selected bond lengths (Å) and angles (deg): Ga(1)−Ga(2), 2.470(4); Ga(1)−C(1), 1.990(2); Ga(2)−C(31), 1.983(3); Ga(1)−C(63), 2.081(4); Ga(2)−C(61), 2.037(4); C(61)−C(62), 1.570(6); C(61)−C(65), 1.514(5); C(62)−C(63), 1.573(6); C(62)−C(67), 1.514(7); C(65)−C(66), 1.501(8); C(66)−C(67), 1.483(6); C(1)−Ga(1)−Ga(2), 141.66(4); C(1)−Ga(1)−C(63), 129.21(1); Ga(2)−Ga(1)−C(63), 87.80(12); C(31)−Ga(2)−Ga(1), 141.78(4); C(31)−Ga(2)−C(61), 121.8(12); C(61)−Ga(2)−Ga(1), 90.47(11).

the Ga−Ga single bond range.[21] The Ga−C distances to the NBD unit [2.037(4) and 2.081(4) Å] are slightly longer than those to the aryl ligand [1.990(2) and 1.983(2) Å]. All of the C−C bonds within the deltacyclane are within the range of single C−C bonds [avg 1.525(6) Å].[22] Each Ga atom is almost trigonal-planar-coordinated, although there is a significant twist about the Ga−Ga bond [C(31)−Ga(1)−Ga(2)−C(1) torsion angle = 55.80(1)°] to accommodate the size of the large ligands, which makes the sum of the angles slightly less than 360° [Ga(1), 358.67(9)°; Ga(2), 354.06(9)°].

We hypothesized that the multiple-bonded digallene would react readily with quadricyclane since the digallene can be considered as a highly π-electrophilic molecule because of the

dx.doi.org/10.1021/ja301247h | J. Am. Chem. Soc. 2012, 134, 7155−7164

relatively low energy of the LUMO (out-of-plane π orbital) in comparison to the LUMO of ethylene. Quadricyclane was independently synthesized by literature methods[23] and added to **1** in hexane at room temperature. An immediate color change from dark-green to bright-orange was observed, and an orange solid was isolated that was identified as **2** by ^{1}H NMR spectroscopy (Scheme 3). The same product is formed through a formal $[2\pi + 2\sigma + 2\sigma]$ cycloaddition in which the digallene is the 2π component. In the presence of excess NBD, **2** is formed as the sole product (as determined by ^{1}H NMR spectroscopy), unlike the group 14 systems (Scheme 3 bottom), and there was no evidence for double $[2\pi + 2\pi]$ cycloaddition of NBD.

UV−vis spectroscopy of **2** revealed three strong absorbances at 226, 303, and 488 nm (ε = 3.3 × 10^4, 8.6 × 10^3, and 3.3 × 10^2 M^{-1} cm^{-1}, respectively). DFT calculations [M06-HF//6-311+G(2df)<Ga>/6-31G(d)<others>] of the molecular orbitals of **2** predicted strong absorbances with values that are in good agreement with the experimental values (Table 1 and Figures S1 and S2 in the Supporting Information). They are a result of transitions between the σ_{Ga-Ga} (HOMO) and σ_{Ga-C} (HOMO−1) and the empty π orbitals centered on the two gallium atoms (LUMO) and π^* orbitals of the ligand (LUMO +1 and LUMO+2), as specified in Table 1.

Table 1. Experimental and Calculated UV−Vis Absorbances and Assigned Transitions for 2−5[a]

	λ/nm (ε/M^{-1} cm^{-1})		
	exptl	calcd[b]	assigned transition
2	226 (3.3 × 10^4)	258 (0.5478)	$\sigma_{Ga-Ga}/\sigma_{Ga-C}$ to p_{Ga}
	303 (8.6 × 10^3)	322 (0.0053)	$\sigma_{Ga-C}/\sigma_{C-C}$ to p_{Ga}
	488 (3.3 × 10^2)	510 (0.0108)	σ_{Ga-Ga} to π^*_{Ar}
3	242 (8.3 × 10^3)	244 (0.1877)	σ_{Ga-C} to $p_{Ga(1)}/\pi^*_{Ar}$
	330 (6.7 × 10^3)	317 (0.0055)	σ_{Ga-C} to $p_{Ga(1)}/\pi^*_{Ar}$
	416 (4.1× 10^3)	384 (0.1058)	σ_{Ga-C} to $p_{Ga(1)}$
4	264 (3.1 × 10^4)	274 (0.2710)	$\sigma_{Ga-C}/\pi_{C=C}$ to π_{Ar}*
	351 (9.6 × 10^3)	364 (0.0801)	$p_{Ga(1)}/p_{C(3)}$
	435 (4.1 × 10^3)	402 (0.0202)	$\sigma_{Ga-C}/\pi_{C=C}$ to $p_{Ga(2)}/p_{C(2)}$
5	262 (1.2 × 10^5)	250 (0.1889)	$\sigma_{Ga-C}/\pi_{C=C}$ to π^*_{Ar}
	350 (2.9 × 10^4)	349 (0.0207)	$\sigma_{Ga-C}/\pi_{C=C}$ to $p_{Ga(1)/Ga(2)}/\pi^*_{C=C}/\pi^*_{Ar}$
	440 (8.0 × 10^3)	412 (0.0167)	$\sigma_{Ga-C}/\pi_{C=C}$ to $p_{Ga(1)/Ga(2)}$

[a]M06-HF//6-311+G(2df) for Ga and 6-31G(d) for all other elements. [b]Calculated oscillator strengths.

We propose that the mechanism of the formal $[2\pi + 2\pi + 2\pi]$ cycloaddition to furnish **2** is similar to the all-carbon version. The reaction may proceed either via a concerted or stepwise nonradical cyclization pathway or by a radical pathway.[24] NBD and quadricyclane differ in that they have FMOs of inverse symmetry,[25] which explains their different reactivities with alkenes. The all-carbon $[2\pi + 2\pi + 2\pi]$ homo-endo-type cyclization reaction[13a,26] between an electron-deficient dienophile and NBD is symmetry-allowed and gives a five-membered ring, whereas the $[2\pi + 2\pi]$ exo-type cyclization reaction resulting in a four-membered ring is symmetry-forbidden (see Scheme 3). These same dienophiles react preferentially to form exo-type products when added to quadricyclane.[27] In contrast, **1** reacts in a homo-endo fashion with both substrates (Scheme 3). Several examples of electrophilic ring-opening reactions of a strained cyclopropane, and more specifically with quadricyclane, are known for all-carbon systems.[28] The relatively low-lying π-type LUMO of **1** can act as an electrophile in the reaction with the strained σ bonds of quadricyclane.

The group 14 analogue, Ar^{iPr_4}SnSnAr^{iPr_4}, reacts with 2 equiv of NBD in an exo-type cyclization, though the known diradicaloid nature of the distannyne may result in a preference for the radical mechanism and preferential double $[2\pi + 2\pi]$ cycloaddition (Scheme 3 bottom).[19]

In the absence of steric restraints, we would expect to see some of the analogous $[2\pi + 2\pi]$ cycloaddition with the digallene, as seen with the group 14 analogues. Since we observed no evidence of this type of reactivity, we propose that the digallene reaction proceeds via a nonradical cyclization mechanism. The reaction with NBD likely proceeds via a concerted 6π cyclization, on the basis of the exclusive formation of the digalladeltacyclane product **2**.

Reaction of 1 with Cyclooctatetraene. Addition of COT to a solution of **1** in hexane at room temperature resulted in an immediate color change from dark-green to bright-yellow. X-ray structural data for the crystals obtained from the solution revealed an addition of a Ar^{iPr_4}GaGaAr^{iPr_4} unit across the COT ring to give **3**, which possesses a central twisted 3,7-cyclooctadiene core with each side bridged by a gallium above and below the carbon ring (see Figure 3). This bonding mode is quite rare and has not previously been seen with addition of neutral COT to a main-group species.[29] Nickel and silver complexes that possess similar twisted ring structures have been reported, but in these the four double bonds of the COT moiety are maintained, and there are two η^2-bound double bonds at each metal atom.[29,30] This formal $[2\pi + 2\pi + 2\pi]$ addition of COT to the digallene is in sharp contrast to the addition of COT to the heavier group 14 analogues Ar^{iPr_4}EEAr^{iPr_4} (E = Ge, Sn), both of which gave a reduction of the polyolefin and resulted in the splitting of the E−E bond and formation of a π-bound inverse-sandwich compound with a planar aromatic C_8H_8 ring (see Scheme 1).[6,7] It also differs from the result reported by Roesky in which the base-stabilized bis(silylene) [PhC(N^{t}Bu)$_2$Si]$_2$ undergoes a [4 + 1] cycloaddition with COT to give a Si−N (ligand) opened structure that maintains a Si−Si bond.[31]

Analysis of the room-temperature ^{1}H and ^{13}C{^{1}H} NMR spectra revealed the fluxional nature of the central ring, since only signals arising from the Ar^{iPr_4} ligands were observed. Variable-temperature NMR spectroscopy permitted the resolution of two broad singlets in the ^{1}H NMR spectrum, one signal for the four olefinic CH groups of the ring and one for the four aliphatic CH groups (Figure 2). Below 273 K, these signals appeared at 2.40 and 4.15 ppm. When the sample was heated to 353 K, the two signals coalesced to one broad singlet at 3.20 ppm that was well-resolved. The ^{13}C{^{1}H} NMR spectrum also showed similar behavior, with the appearance of one olefinic signal at 121.9 ppm and one aliphatic signal at 30.3 ppm upon cooling to 243 K. The ^{1}H−^{13}C correlation for the new peaks was confirmed by low-temperature two-dimensional HSQC NMR spectroscopy (see Figure S5 in the Supporting Information).

The molecular orbitals of **3** were calculated by DFT analysis [M06-HF//6-311+G(2df)<Ga>/6-31G(d)<others>] and the UV−vis absorptions were also predicted (see Figures S3 and S4 in the Supporting Information). The main absorbance, predicted to be at 416 nm, is attributed to the transition from the HOMO, which is centered on the Ga−C σ bonds between gallium and the central carbon ring, to the LUMO, involving the empty π orbital at Ga(1) and the π^* system of the

dx.doi.org/10.1021/ja301247h | J. Am. Chem. Soc. 2012, 134, 7155−7164

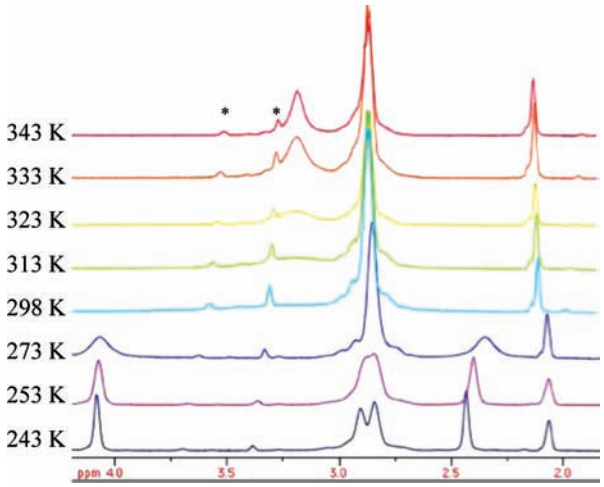

Figure 2. Stacked plot of the aliphatic region of the ^{1}H NMR spectra of **3** in C_7D_8. A small amount of $\mathbf{3}^{iso}$ was present, as indicated by peaks labeled with *.

terphenyl ligand (Figure S3 in the Supporting Information). The other transitions, predicted to be at 244 and 317 nm, are from the HOMO to the LUMO+1 (aryl ligand π^* orbital) and the HOMO to the LUMO+2 [empty π orbital on Ga(2)]. The predicted and experimental absorption bands of **3** were in good agreement (see Table 1).

The solid-state structure of **3** showed two crystallographically independent molecules in the unit cell (Figure 3). This is consistent with the fluxional behavior of the central ring seen in the ^{1}H NMR spectrum. There are two slightly different orientations of the central ring, which result in different interactions with gallium. There is an increased twist in the ring, with short Ga(1)−C(34), Ga(1A)−C(33), Ga(2)−C(74), and Ga(2A)−C(77) contacts [2.454(5), 2.538(5), 2.508(4), and 2.405(5) Å, respectively] as a result. The gallium p orbital can interact with the remaining π bond of the resultant 1,5-cyclooctadiene ring. The bond distances between gallium and the ligand [avg 1.955(14) Å] as well as gallium and the central 1,5-cyclooctadiene (COD) ring [avg 1.988(2) Å] are within the expected range for Ga−C single bonds,[21] though the distances from the central ring to Ga are slightly longer than the aryl−Ga distances in the starting compound **1**.[12] The two C−C bonds at either end of the central ring remain unbroken double bonds [avg 1.345(8) Å], while the bridging C−C bonds are slightly longer [avg 1.563(5) Å] than the rest of the C−C single bonds in the ring [1.485(6)−1.534(6) Å]. The cross-ring Ga···Ga distance of 3.880(4) Å is too long for significant bonding. The geometry at each gallium is nearly perfectly trigonal-planar, since the sum of the angles at gallium are 359.7(1)° and 360.0(1)°.

The tub shape of free COT is known to prevent a planar alignment of at least one diene unit, making COT an ineffective 4π component in $[4\pi + 2\pi]$ cycloaddition reactions with alkenes. The formation of a highly reactive valence tautomer of COT, bicyclo[4.2.0]octa-2,4,7-triene, which does possess a planar 4π component, has been shown to be present in equilibrium in solution.[32] It is possible that **1** can react in a $[2\pi + 2\pi]$ radical fashion with the cyclobutene fragment of this isomer to give a cycloadduct intermediate ($\mathbf{3}^{iso}$) or equally in a $[4\pi + 2\pi]$ fashion (Scheme 4). A $[6\pi + 2\pi]$ cyclization with COT would furnish intermediate $\mathbf{3}^{iso}$ via a nonradical pathway and could also lead to **3**. A [1,3]-shift of the $Ar^{iPr_4}Ga$ unit

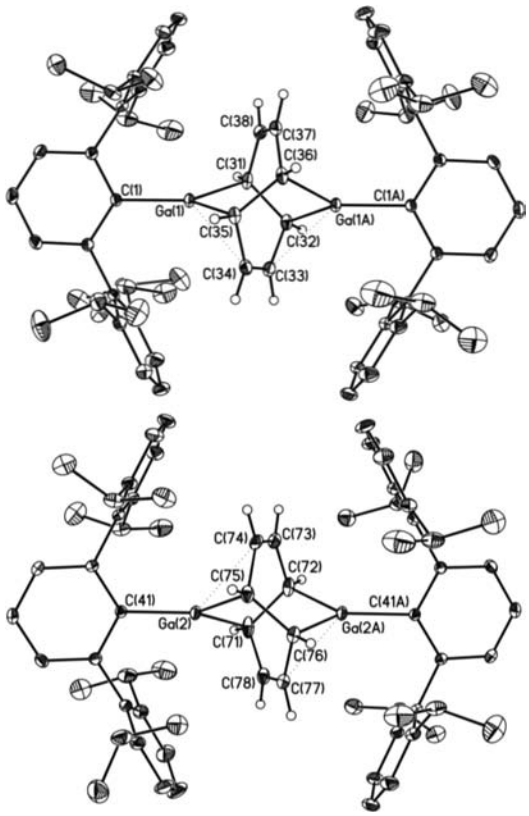

Figure 3. Thermal ellipsoid (30%) plot of the two crystallographically independent molecules of **3**. Selected H atoms, a symmetry-related second central COD ring for each independent molecule, and isopropyl group disorder are not shown. Selected bond lengths (Å): Ga(1)···Ga(1A), 3.880(4); Ga(1)−C(1), 1.959(9); Ga(1)−C(31), 2.005(3); Ga(1)···C(34), 2.454(5); Ga(1)−C(35), 1.999(3); Ga(1A)···C(32), 1.954(3); Ga(1A)−C(36), 2.005(3); Ga(1A)···C(33), 2.528(5); Ga(2)−C(41), 1.9505(14); Ga(2)−C(71), 2.022(3); Ga(2)···C(74), 2.508(4); Ga(2)−C(75), 1.974(3); Ga(2A)−C(72), 2.034(3); Ga(2A)−C(76), 1.916(3); Ga(2A)···C(77), 2.405(5); C(31)−C(32), 1.566(5); C(32)−C(33), 1.509(6); C(33)−C(34), 1.354(9); C(34)−C(35), 1.500(7); C(35)−C(36), 1.564(4); C(36)−C(37), 1.493(7); C(37)−C(38), 1.346(9); C(38)−C(31), 1.488(8); C(71)−C(72), 1.561(5); C(72)−C(73), 1.508(7); C(73)−C(74), 1.291(8); C(74)−C(75), 1.534(6); C(75)−C(76), 1.560(4); C(76)−C(77), 1.485(7); C(77)−C(78), 1.390(7); C(71)−C(78), 1.485(6).

Scheme 4. Possible Mechanism for the Formation of 3 and Isomerization Back to the Cyclization Adduct $\mathbf{3}^{iso}$

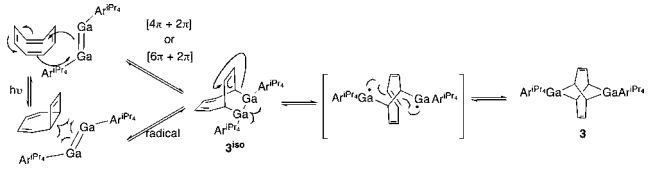

(which would proceed in an antarafacial fashion under thermal conditions for all-carbon systems) and homolytic cleavage of the Ga−Ga bond followed by reaction across the central olefin could give **3**. Crystals of **3** are stable under a N_2 atmosphere, but we observed gradual isomerization of **3** in solution by ^{1}H NMR spectroscopy. The isomerization gives an equilibrium mixture of **3** and a product with four magnetically distinct ^{1}H signals for the ring protons. We were led to the conclusion that this isomer could be the intermediate $\mathbf{3}^{iso}$ in the mechanistic pathway shown (Scheme 4).

dx.doi.org/10.1021/ja301247h | J. Am. Chem. Soc. 2012, 134, 7155−7164

Two-dimensional NMR spectroscopy (COSY and HSQC) supported the assignment for the structure of the isomeric product, although additional definitive structural characterization of this isomer could not be obtained (see the Supporting Information) since the structure of $\mathbf{3}^{iso}$ could not be confirmed by X-ray crystallographic analysis. Other supporting evidence for the structure of $\mathbf{3}^{iso}$ is based on a comparison with the related [6π + 2π] metal-promoted cyclization observed with alkenes and alkynes.[3,33] We also observed the formation of free COT (5.77 ppm) in the ^{1}H NMR spectrum of the sample after the solution was stored for several days at room temperature under a nitrogen atmosphere. The reformation of **1** was difficult to confirm by ^{1}H NMR spectroscopy because the isopropyl methine and diastereotopic methyl resonances overlapped and were obscured by the significantly more intense resonances of **3**, which was also present. However, the reappearance of COT supports the proposed mechanism and the overall reversibility of these cyclization reactions.

The product **3** could potentially form via a radical mechanism with two double bonds of COT without invoking an initial cyclization reaction. However, treatment of **1** with 1,5-cyclooctadiene gave no apparent color change, and no reaction could be detected by ^{1}H NMR spectroscopy, even under more forcing conditions (65 °C, 3 h). Treatment of **1** with 1,4-cyclohexadiene also did not afford a reaction under similar conditions (85 °C, 3 h). These results indicate that the conjugation of the cyclic polyolefins is crucial for reaction with the digallene, ruling out the possibility for a [2π + 2π + 2π] reaction with cyclic nonconjugated polyolefins.

Reaction of 1 with Cyclopentadiene. Weidenbruch and co-workers previously showed that a tetra-*tert*-butyldisilene (generated in situ from the photolysis of hexa-*tert*-butylcyclotrisilane) reacted with CpH to provide the [4π + 2π] cycloadduct along with other unidentified products.[34] We treated **1** with CpH and observed an immediate color change from green to orange. Concentration and cooling of the solution to ca. −18 °C for 3 weeks afforded X-ray-quality crystals of **4**, and the structure of **4** is shown in Figure 4.

The Ga−Ga bond is maintained [2.4534(7) Å] and is within the range expected for a Ga−Ga single bond.[21] The cyclopentene fragment is bound to the $Ar^{iPr_4}GaGaAr^{iPr_4}$ moiety by three short contacts, Ga(1)−C(1) [2.042(2) Å], Ga(2)−C(3) [2.444(3) Å], and Ga(2)−C(4) [2.076(2) Å]. The average aryl−Ga distance [1.989(2) Å] is shorter than the Ga−ring carbon distance seen in all of the previous structures. Within the ring, the shortest distance involves C(2)−C(3) [1.338(4) Å], as would be expected if a [4π + 2π] reaction had taken place. The distances for C(1)−C(2) and C(3)−C(4) are 1.479(4) and 1.426(4) Å, respectively, which are significantly shorter than normal C−C single bonds (ca. 1.54 Å) but longer than C=C double bonds (ca. 1.33 Å).[22] These single bonds are likely shortened as a result of an additional interaction and short contact of C(3) with Ga(2). The two remaining C−C bonds in the ring, C(4)−C(5) [1.514(4)] Å and C(1)−C(5) [1.546(4) Å], are within the range expected for C−C single bonds.[22] The large terphenyl rings are twisted [C(6)−Ga(1)−Ga(2)−C(36) torsion angle = 26.58(14)°] to accommodate the cyclopentene ring within the isopropyl groups. The sum of the angles at each Ga is consistent with trigonal-planar coordination [Ga(1), 359.37(6)°; Ga(2), 359.69(7)°].

The ^{1}H NMR spectrum of **4** is complicated as a result of its lower symmetry arising from the way in which the cyclopentenyl ring is bound. In the starting $Ar^{iPr_4}GaGaAr^{iPr_4}$, the diastereotopic methyl groups appear as a pair of overlapping doublets at 1.08 ppm and the ligand isopropyl methine as a septet at 2.96 ppm. In **4**, however, the signals for the methyl and methine groups appear as complex multiplets at ca. 1.1 and 2.9 ppm, respectively. They also overlap with the aliphatic CH and CH_2 groups of the cyclopentene ring. A distinct signal attributable to the olefinic CH groups of the cyclopentene appear as a singlet at 5.89 ppm. The $^{13}C\{^1H\}$ NMR spectrum displays seven aliphatic signals that are also indicative of the lower symmetry of the ligand environment but also possesses a new olefinic signal at 120.5 ppm attributable to the cyclopentene ring. The UV−vis spectrum of **4** revealed strong absorptions at 264 nm ($\varepsilon = 3.1 \times 10^4$ M^{-1} cm^{-1}), 351 nm ($\varepsilon = 9.6 \times 10^3$ M^{-1} cm^{-1}), and 435 nm ($\varepsilon = 4.1 \times 10^3$ M^{-1} cm^{-1}). DFT calculations [(M06-HF//6-311+G(2df)<Ga>/6-31G(d)<others>] on **4** revealed that the HOMO is centered on the Ga−C_{ring} σ bonds and the C=C π bonds in the ring (Figures S7 and S8 in the Supporting Information). The absorbances predicted by the DFT calculations involve transitions from the HOMO to the LUMO and LUMO+1 [involving the empty p orbitals at Ga(1) and Ga(2)] and the LUMO+2 (ligand π^*_{Ar}) and agree well with the experimental results (Table 1).

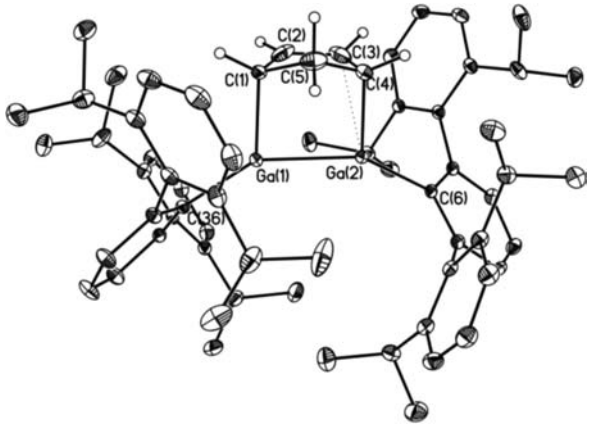

Figure 4. Thermal ellipsoid (30%) plot of **4**. A pentane solvent molecule and ligand H atoms are not shown. Selected bond lengths (Å) and angles (deg): Ga(1)−Ga(2), 2.4534(7); Ga(1)−C(1), 2.042(2); Ga(2)···C(3), 2.444(3); Ga(2)−C(4), 2.076(2); Ga(2)−C(6), 1.995(2); Ga(1)−C(36), 1.983(2); C(1)−C(2), 1.479(4); C(2)−C(3), 1.338(4); C(3)−C(4), 1.426(4); C(4)−C(5), 1.514(4); C(1)−C(5), 1.546(4); C(1)−Ga(1)−C(36), 121.95(8); Ga(2)−Ga(1)−C(36), 149.12(5); C(1)−Ga(1)−Ga(2), 88.31(6); C(6)−Ga(2)−C(4), 121.01(9); C(6)−Ga(2)−C(3), 119.47(8); C(4)−Ga(2)−C(3), 35.61(10); C(6)−Ga(2)−Ga(1), 148.82(5); C(4)−Ga(2)−Ga(1), 88.84(7); C(3)−Ga(2)−Ga(1), 81.47(6).

Finally, we note that the reaction of **1** with CpH stands in sharp contrast to that of its germanium counterpart $Ar^{iPr_4}GeGeAr^{iPr_4}$, which releases H_2 and forms $Ar^{iPr_4}Ge(\eta^5\text{-}C_5H_5)$.[35] In effect, the germanium species behaves as a reducing agent analogous to sodium, whereas **1** behaves as a simple 2π electron moiety in its interaction with the 4π electrons of CpH.

Reaction of 1 with 1,3,5-Cycloheptatriene. We then tested a larger conjugated ring to determine whether it would undergo the same [4π + 2π] reaction or an [nπ + 2π] cyclization, where *n* is the number of conjugated π electrons in the ring. In comparison, the [6π + 2π] cycloaddition of CHT with alkenes has been shown to proceed under transition-metal catalysis conditions with iron(0),[33a] chromium(0), and cobalt(0) complexes of CHT[3,33b,36] as well as with

dx.doi.org/10.1021/ja301247h | J. Am. Chem. Soc. 2012, 134, 7155−7164

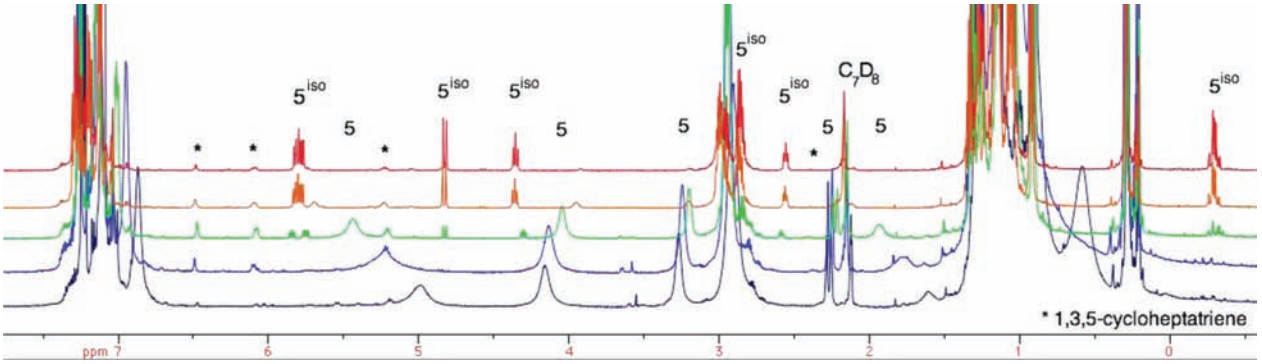

Figure 5. Stacked plot of the ^{1}H NMR spectra recorded in C_7D_8 illustrating the isomerization of **5** to **5**^{iso} with the appearance of free CHT (*). Bottom to top: 313, 333, 353, 373, and 373 K after 10 min.

$TiCl_4$·Et_2AlCl as a catalyst.[37] The [6π + 2π] cyclization has been shown to proceed in a stepwise manner to avoid symmetry restrictions. The use of a catalyst allows the symmetry restrictions to be lifted by altering the symmetry of the HOMO, allowing the complex to undergo pericyclic reactions and/or by enhancing the rate of a multistep reaction.

Reaction of **1** with CHT in hexane resulted in an immediate color change of the solution from dark-green to dark-red. The ^{1}H NMR spectrum displayed five resonances that could be assigned to the ring protons (Figure 5 bottom), which allowed us to make a tentative assignment of the cyclized adduct as product **5**. However, some of the signals in the spectrum were broad, so variable-temperature ^{1}H NMR spectroscopy was undertaken. At 313 K, two broad resonances at 4.2 and 5.1 ppm were assigned to the four olefinic C*H* groups, and the signal at 3.3 ppm was assigned to the CH groups adjacent to the Ga atoms in **5**. A distinctive doublet at 2.3 ppm was assigned to the bridgehead proton oriented toward the diene moiety, with a large $^2J_{HH}$ coupling constant of 16.8 ppm. The bridgehead proton oriented toward the Ga−Ga moiety at 1.57 ppm also had a large coupling, but it was not well resolved. When a sealed C_7D_8 solution of **5** was cooled to 253 K, however, the olefinic signals remained broad (data not shown). The solution was then gradually heated to 373 K and held at that temperature for 10 min (Figure 5 top). The disappearance and temperature-dependent drift in the chemical shift for the broad resonances of **5** was observed. Free CHT signals were also identified in the spectra between 353 and 373 K. The appearance of seven well-resolved signals was observed (the eighth signal was determined to be buried beneath the isopropyl methine multiplet by integration and 2D COSY NMR spectroscopy (Figure S11 in the Supporting Information). A color change from red to yellow accompanied the gradual appearance of seven well-resolved resonances. Cooling of the sample to room temperature did not restore the red color or the original ^{1}H NMR spectrum. Instead, the spectrum indicated the formation of the isomer **5**^{iso}, which is likely the thermodynamically favored product. The isomerized product **5**^{iso} showed an unsymmetrical and unique environment for each proton in the ring by ^{1}H NMR spectroscopy.

On the basis of the NMR data, we propose that an initial [6π + 2π] cycloaddition occurs to form **5**, which is the kinetic product. At elevated temperatures, the cyclization reaction is reversible, producing free CHT in solution, which can then recyclize via a [4π + 2π] cyclization to give the thermodynamically preferred structural isomer, **5**^{iso} (Scheme 5). It is also possible that a [1,3]-sigmatropic Ar^{iPr_4}Ga shift may cause the

Scheme 5. Proposed Mechanism for the Formation of 5 and the Isomerization to 5^{iso}

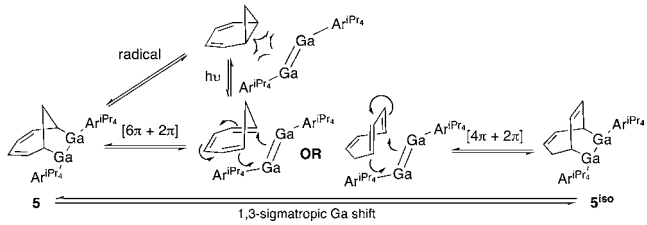

isomerization from **5** to **5**^{iso}, although the steric bulk of the terphenyl ligand makes this possibility unlikely. As seen with the COT cyclization, CHT is known to form a highly strained bicyclic species, norcaradiene,[38] which could also potentially undergo a radical-mediated cyclization to give **5**.

Concentration and cooling of a diethyl ether solution of **1** and excess CHT to −18 °C afforded X-ray-quality crystals. The solid-state structure revealed that the [4π + 2π] cyclization product **5**^{iso} had preferentially crystallized, as evidenced by the formation of the Ga(1)−C(61) and Ga(2)−C(65) single bonds (Figure 6).

The ring bond distances revealed that double bonds are present between C(63)−C(64) [1.367(3) Å] and C(66)−C(67) [1.337(4) Å] after the cyclization, indicative of a 1,4-cycloheptadienyl fragment that is bound to the two galliums of Ar^{iPr_4}GaGaAr^{iPr_4} at the C(61) and C(66)/C(65) atoms. The C(66)−C(67) distance [1.337(4) Å] is slightly shorter than that in the other C−C double bond in the ring [C(63)−C(64), 1.367(3) Å] as a result of the Ga(2)−C(66) interaction, which is relatively short [2.352(3) Å]. The Ga(2)−C(65) and Ga(1)−C(61) distances [2.219(4) and 2.020(7) Å, respectively] are reasonable for alkyl Ga−C single bonds[21] but longer than the Ga−aryl distances [1.985(3) and 1.983(6) Å] seen in the other structures **2**, **3**, and **4**. All of the other C−C bonds in the ring are single bonds. The Ga(1)−Ga(2) bond distance is within the expected range for a Ga−Ga single bond.[21] The terphenyl ligands are in an approximately cis orientation as a result of bonding to the cycloheptadiene ring. The cycloheptadiene ring is positioned at nearly right angles with respect to the Ga−Ga bond [C(65)−Ga(2)−Ga(1) = 97.18(6)° and C(61)−Ga(1)−Ga(2) = 95.63(5)°]. The sums of the angles at the two gallium atoms [359.9(5) and 359.3(6)°] indicate near trigonal-planar geometry, discounting the weak interaction to C(66).

The UV−vis spectrum of **5**^{iso} revealed strong absorptions at 440 nm ($\varepsilon = 8.0 \times 10^4$ M^{-1} cm^{-1}), 350 nm ($\varepsilon = 2.0 \times 10^4$ M^{-1}

dx.doi.org/10.1021/ja301247h | J. Am. Chem. Soc. 2012, 134, 7155−7164

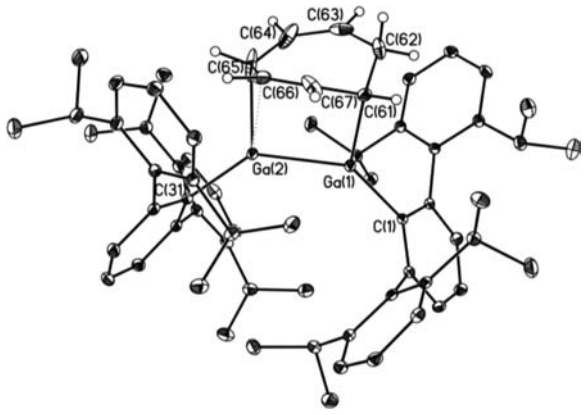

Figure 6. Thermal ellipsoid (30%) plot of $\mathbf{5}^{iso}$. Ligand H atoms and a cocrystallized diethyl ether solvent molecule are not shown. Selected bond lengths (Å) and angles (deg): Ga(1)−Ga(2), 2.469(3); Ga(1)−C(1), 1.985(2); Ga(2)−C(31), 1.983(6); Ga(1)−C(61), 2.020(7); Ga(2)−C(65), 2.219(4); Ga(2)−C(66), 2.352(3); C(61)−C(62), 1.507(3); C(62)−C(63), 1.447(3); C(63)−C(64), 1.367(3); C(64)−C(65), 1.479(4); C(65)−C(66), 1.398(4); C(66)−C(67), 1.337(4); C(67)−C(61), 1.494(3); C(1)−Ga(1)−Ga(2), 136.48(4), C(1)−Ga(1)−C(61), 128.89(6); C(31)−Ga(2)−Ga(1), 138.13(5); C(31)−Ga(2)−C(65), 123.98(7); Ga(1)−Ga(2)−C(65), 97.18(6); Ga(2)−Ga(1)−C(61), 118.09(14).

cm^{-1}) and 265 nm ($\varepsilon = 1.2 \times 10^5\ M^{-1}\ cm^{-1}$). DFT calculations [M06-HF//6-311+G(2df)<Ga>/6-31G(d)<others>] on **5** afforded molecular orbitals similar to those of **4**, with the HOMO centered on the Ga−C_{ring} bonds with a significant contribution from the π bonds of the ring (see Figures S9 and S10 in the Supporting Information). In this structure, the DFT-predicted absorbances are due to transitions from the HOMO to the LUMO [empty p orbitals on Ga(1) and Ga(2)], LUMO+1 (ring $\pi^*_{C=C}$), and LUMO+2 (ligand π^*_{Ar}) and agree moderately well with the experimental results (Table 1).

GENERAL REMARKS AND CONCLUSIONS

As has been shown above, the heavier group 13 dimetallene $Ar^{iPr_4}GaGaAr^{iPr_4}$ (**1**) participates in cyclization reactions with a range of cyclic polyolefins, including CpH, CHT, COT, NBD, and the strained polycycle quadricyclane, that are akin to the corresponding cyclization reactions with alkenes but proceed under much milder conditions. Furthermore, the dimetallene either reacts with polyolefins that are unreactive toward the corresponding heavier group 14 analogues (in the case of CHT) or reacts to give products that are significantly different. For example, $Ar^{iPr_4}EEAr^{iPr_4}$ (E = Ge, Sn) give inverse-sandwich products when reacted with COT,[6,7] π complexes along with H_2 release when reacted with CpH,[35] and double [2π + 2π] cycloaddition products with NBD.[19] On the basis of the products formed, we postulate that the group 13 analogues are more likely to react in a nonradical fashion, whereas the heavier group 14 analogues are more diradicaloid character[39] making them more prone to undergo reactive pathways not seen for carbon. **1** reacts much more readily than olefins and without the use of transition-metal catalysts or forcing conditions.

The Woodward−Hoffmann rules for all-carbon cycloadditions predict that both [2π + 2π] and [6π + 2π] cycloadditions are symmetry-forbidden, while the [4π + 2π] Diels−Alder and [2π + 2π + 2π] homo-Diels−Alder reactions are symmetry-allowed under thermal conditions.[40] Unlike the FMOs for simple alkenes, which consist of a π-type HOMO and π^*-type LUMO, the calculated FMOs for the heavier group 13 multiple-bonded analogues are both of π symmetry, although their overall shapes are very different (Figure 7).

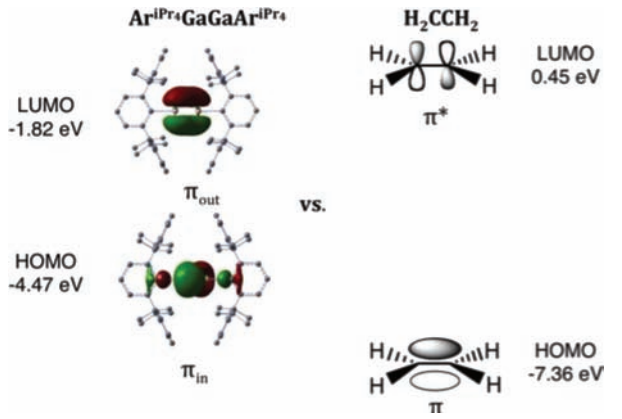

Figure 7. Illustration of the FMOs of **1** calculated using DFT [B3PW91/6-311+G(2df) for Ga, 6-31G(d) other atoms; contour value = 0.04] compared with the FMOs of ethylene.[12]

This $\pi-\pi$ FMO arrangement differs not only from that of the olefins but also from that of the neighboring heavier group 14 analogues, whose FMOs are of $\pi-n_+$ symmetry. In essence, the heavier group 13 dimetallene FMOs can interact with *both* the HOMO and LUMO FMOs of the polyolefins, regardless of their symmetry. This difference has broad implications, as these systems are less restricted by the Woodward−Hoffmann symmetry rules, specifically as applied to predict cycloaddition reactivity. This is illustrated in the reactions of NBD and quadricyclane with **1**. These two substrates present a similar steric profile, but their FMOs have been shown to be of inverse symmetry.[25] Different products are obtained in the reactions of NBD and quadricyclane with olefins, since the olefins obey the orbital symmetry restrictions of the Woodward−Hoffmann rules. Olefins react with NBD to give the homo-endo cyclization product but react with quadricyclane to give the exo-type product. The $\pi-\pi$ symmetry of the FMOs of **1** allow it to react with both substrates to give the same homo-endo digalladeltacyclane product, regardless of the Woodward−Hoffmann restrictions.

This effect is also demonstrated by the [6π + 2π] cyclization reactions studied. The thermal cyclization reaction of alkenes with 6π polyolefins is symmetry-forbidden, but it has been shown to proceed in the presence of several group 10 metal catalysts.[3,33b,36,37] The presence of electron-withdrawing groups in the olefin lowers the energy of the π^* LUMO, enhancing the d−π^* back-bonding interaction from the zero-valent metal to the olefin and increasing the reactivity. As we have shown, **1** reacts readily with CHT and COT without the need for a transition-metal catalyst.

DFT calculations showed that, in addition to significant differences in the symmetry of the FMOs, there are substantial energy differences between the FMOs of 2π alkenes and the heavier group 13 analogues. The heavier group 13 analogues are in effect more electron-deficient *and* more electron-rich reactive partners than simple alkenes (cf. Figure 7). This effect has previously been implicated in the ready reactivity of disilenes.[41] The increased reactivity of the group 13 dimetallene is also due to the relatively weak Ga−Ga bonding and the calculated HOMO−LUMO gap of 2.7 eV (ca. 62 kcal mol^{-1}),

dx.doi.org/10.1021/ja301247h | J. Am. Chem. Soc. 2012, 134, 7155−7164

which is significantly smaller than the value of 7.8 eV for ethylene (Figure 7). This effect is evident experimentally, as an increase in reactivity is seen for alkenes that are activated toward cycloaddition reactions by the presence of strongly electron-withdrawing groups. Tetracyanoethylene is the only alkene that undergoes $[2\pi + 2\pi + 2\pi]$ cyclization with NBD and $[2\pi + 2\sigma + 2\sigma]$ cyclization with quadricyclane without the need for transition-metal catalysis.[27a,42]

Periselectivity is a concern in carbon chemistry, since higher-order cyclization reactions are known to afford complex mixtures of products due to multiple irreversible competitive pathways (i.e., $[2\pi + 2\pi]$ vs $[4\pi + 2\pi]$ vs $[6\pi + 2\pi]$).[3] While we observed different cyclization products for the reactions of **1** with the larger cyclic polyolefins, we also observed temperature-dependent interconversion between them. In the reaction of **1** with CHT, both $[6\pi + 2\pi]$ and $[4\pi + 2\pi]$ cyclization products (**5** and $\mathbf{5}^{iso}$, respectively) were observed. The proposed mechanism for this reaction relies on the reversibility of the cyclizations, where complete isomerization of the initially formed $[6\pi + 2\pi]$ product **5** occurred to form the $[4\pi + 2\pi]$ adduct $\mathbf{5}^{iso}$ at elevated temperatures. CpH also undergoes a $[4\pi + 2\pi]$ cyclization with **1** to afford **4**. These $[4\pi + 2\pi]$ and $[6\pi + 2\pi]$ cyclization products are structurally analogous to those of the all-carbon systems.

In the reaction of **1** with COT, the $[4\pi + 2\pi]$ and $[6\pi + 2\pi]$ cyclization pathways are indistinguishable, as they both afford the same product, **3**. Isomerization of **3** was observed, however, yielding the structural isomer $\mathbf{3}^{iso}$ in solution over time. This onward isomerization is not seen in the all-carbon cyclization product, indicating that even after cyclization, the Ga−Ga bond remains highly reactive, likely as a result of the remaining low-lying LUMO, which consists of empty π-type orbitals at each gallium.

Singlet carbenes have been shown to react with 2π equivalents to form stable cyclopropanes.[43] In addition, the heavier element singlet silylenes[44] and germylenes[45] have both been shown to undergo preferential $[2 + 1]$ and $[4 + 1]$ cyclizations. We see no evidence for $[n + 1]$ cyclization products (where $n = 2, 4, 6$), which would arise from the reaction of a $Ar^{iPr_4}Ga$: monomer with an alkene, diene, or triene. Nevertheless, a mechanism involving a multistep reaction between cyclic polyolefins and 2 equiv of $Ar^{iPr_4}Ga$: monomer remains a possibility. We also highlight that all of the structures obtained possess two "$Ar^{iPr_4}Ga$" fragments, and compounds **2**, **4**, and $\mathbf{5}^{iso}$ maintain an intact Ga−Ga bond. Despite the fact that the digallene **1** is extensively dissociated to $Ar^{iPr_4}Ga$: monomers in solution, the experimental data indicate that the digallene form is much more reactive towards olefins than the monomer. Further investigations regarding the mechanistic details of these cycloaddition reactions are underway.

In summary, we have shown that the double-bonded digallene **1** behaves as a highly reactive heavy alkene analogue in cyclization reactions with polyolefins, including (i) the $[4\pi + 2\pi]$ reaction with CpH and CHT, (ii) the $[6\pi + 2\pi]$ cyclization reaction with CHT and COT, and (iii) the $[2\pi + 2\sigma + 2\sigma]$ and $[2\pi + 2\pi + 2\pi]$ reactions with quadricyclane and NBD, respectively, to furnish digalladeltacyclane. The higher-order ring structures obtained are only achievable under catalytic conditions in the all-carbon system or with highly electron-deficient alkenes. The increased reactivity is attributed to the smaller HOMO−LUMO gap and the π−π symmetry of the FMOs of **1**, which are in sharp contrast to the FMOs of alkenes, alkynes, and their heavier group 14 element analogues. The increased electrophilicity and nucleophilicity of these species and their propensity to undergo nonradical cyclization pathways make them closer analogues to the all-carbon system than the heavier group 14 analogues, which behave in a manner more consistent with significant diradicaloid character.[39]

■ ASSOCIATED CONTENT

Ⓢ Supporting Information

Calculated structures, molecular orbital figures for **2**−**5**, 2D COSY and HSQC experiments, and X-ray crystallographic data (CIF) for **2**−**5**. This material is available free of charge via the Internet at http://pubs.acs.org.

■ AUTHOR INFORMATION

Corresponding Author

pppower@ucdavis.edu

Notes

The authors declare no competing financial interest.

■ ACKNOWLEDGMENTS

We thank the U.S. Department of Energy (DE-FG02-07ER46475) for funding and the Natural Sciences and Engineering Research Council of Canada (NSERC) for a postdoctoral fellowship. J.-D.G. and S.N. are grateful for a Grant-in-Aid for Specially Promoted Research from the MEXT of Japan.

■ REFERENCES

(1) Diels, O.; Alder, K. *Justus Liebigs Ann. Chem.* **1928**, *460*, 98.
(2) Lautens, M.; Edwards, L. G.; Tam, W.; Lough, A. J. *J. Am. Chem. Soc.* **1995**, *117*, 10276.
(3) Rigby, J. H.; Ateeq, H. S.; Charles, N. R.; Henshilwood, J. A.; Short, K. M.; Sugathapala, P. M. *Tetrahedron* **1993**, *49*, 5495.
(4) (a) Fleming, I. *Frontier Orbitals and Organic Chemical Reactions*; Wiley: London, 1976. (b) Fleming, I. *Pericyclic Reactions*; Oxford University Press: Oxford, U.K., 1999.
(5) (a) Ojima, I.; Tzamarioudaki, M.; Li, Z.; Donovan, R. J. *Chem. Rev.* **1996**, *96*, 635. (b) Lautens, M.; Klute, W.; Tam, W. *Chem. Rev.* **1996**, *96*, 49.
(6) Summerscales, O. T.; Wang, X.; Power, P. P. *Angew. Chem., Int. Ed.* **2010**, *49*, 4788.
(7) Summerscales, O. T.; Jiménez-Halla, J. O. C.; Merino, G.; Power, P. P. *J. Am. Chem. Soc.* **2011**, *133*, 180.
(8) Jones, C.; Stasch, A. In *The Group 13 Metals Aluminum, Gallium, Indium and Thallium: Chemical Patterns and Peculiarities*; Aldridge, S., Downs, A. J., Eds.; Wiley: Chichester, U.K., 2011.
(9) Hardman, N. J.; Wright, R. J.; Phillips, A. D.; Power, P. P. *J. Am. Chem. Soc.* **2003**, *125*, 2667.
(10) Caputo, C. A.; Zhu, Z.; Brown, Z. D.; Fettinger, J. C.; Power, P. P. *Chem. Commun.* **2011**, *47*, 7506.
(11) Hardman, N. J.; Wright, R. J.; Phillips, A. D.; Power, P. P. *Angew. Chem., Int. Ed.* **2002**, *41*, 2842.
(12) Zhu, Z.; Fischer, R. C.; Ellis, B. D.; Rivard, E.; Merrill, W. A.; Olmstead, M. M.; Power, P. P.; Guo, J. D.; Nagase, S.; Pu, L. *Chem.—Eur. J.* **2009**, *15*, 5263.
(13) (a) Tabushi, I.; Yamamura, K.; Yoshida, Z. *J. Am. Chem. Soc.* **1972**, *94*, 787. (b) Domingo, L. R.; Saéz, J. A.; Zaragozá, R. J.; Arnó, M. *J. Org. Chem.* **2008**, *73*, 8791. (c) Jones, G. A.; Shephard, M. J.; Paddon-Row, M. N.; Beno, B. R.; Houk, K. N.; Redmond, K.; Carpenter, B. K. *J. Am. Chem. Soc.* **1999**, *121*, 4334.
(14) Noyori, R.; Umeda, I.; Kawauchi, H.; Takaya, H. *J. Am. Chem. Soc.* **1975**, *97*, 812.
(15) Hall, H. K. J. *J. Org. Chem.* **1960**, *25*, 42.

(16) Paquette, L. A.; Kesselmayer, M. A.; Künzer, H. *J. Org. Chem.* **1988**, *53*, 5183.
(17) Goldstein, M. J.; Natowsky, S.; Heilbronner, E.; Hornung, V. *Helv. Chim. Acta* **1973**, *56*, 294.
(18) Hoffmann, R. *Acc. Chem. Res.* **1971**, *4*, 1.
(19) Peng, Y.; Ellis, B. D.; Wang, X.; Fettinger, J. C.; Power, P. P. *Science* **2009**, *325*, 1668.
(20) (a) Lautens, M.; Lautens, J. C.; Smith, A. C. *J. Am. Chem. Soc.* **1990**, *112*, 5627. (b) Lautens, M.; Tam, W.; Lautens, J. C.; Edwards, L. G.; Crudden, C. M.; Smith, A. C. *J. Am. Chem. Soc.* **1995**, *117*, 6863.
(21) Uhl, W. *Chem. Soc. Rev.* **2000**, *29*, 259.
(22) Wells, A. F. *Structural Inorganic Chemistry*; Clarendon Press: Oxford, U.K., 1984.
(23) Smith, C. D. *Org. Synth.* **1971**, *51*, 133.
(24) Moilanen, J.; Power, P. P.; Tuononen, H. M. *Inorg. Chem.* **2010**, *49*, 10992.
(25) (a) Hoffmann, R.; Heilbronner, E.; Gleiter, R. *J. Am. Chem. Soc.* **1970**, *92*, 706. (b) Bischof, P.; Hashmall, J. A.; Heilbronner, E.; Hornug, V. *Helv. Chim. Acta* **1969**, *52*, 1745. (c) Martin, H.-D.; Heller, C.; Haselbach, E.; Lanyjova, Z. *Helv. Chim. Acta* **1974**, *57*, 465. (d) Haselbach, E.; Martin, H.-D. *Helv. Chim. Acta* **1974**, *57*, 472.
(26) Lautens, M.; Edwards, L. G. *J. Org. Chem.* **1991**, *56*, 3761.
(27) (a) Blomquist, A. T.; Meinwald, Y. C. *J. Am. Chem. Soc.* **1959**, *81*, 667. (b) Yamaguchi, R.; Ban, M.; Kawanisi, M.; Osawa, E.; Jaime, C.; Buda, A. B.; Katsumata, S. *J. Am. Chem. Soc.* **1984**, *106*, 1512. (c) Smith, C. D. *J. Am. Chem. Soc.* **1966**, *88*, 4273.
(28) Cassar, L.; Halpern, J. *J. Chem. Soc. D* **1970**, 1082.
(29) Bach, I.; Pörschke, K.-R.; Proft, B.; Goddard, R.; Kopiske, C.; Krüger, C.; Rufińska, A.; Seevogel, K. *J. Am. Chem. Soc.* **1997**, *119*, 3773.
(30) Mak, T. C. W. *J. Organomet. Chem.* **1983**, *246*, 331.
(31) Sen, S. S.; Khan, S.; Kratzert, D.; Roesky, H. W.; Stalke, D. *Eur. J. Inorg. Chem.* **2011**, 1370.
(32) (a) Huisgen, R.; Meitzsch, F. *Angew. Chem., Int. Ed. Engl.* **1964**, *3*, 83. (b) Paquette, L. A. *Tetrahedron* **1975**, *31*, 2855.
(33) (a) Davis, R. E.; Dodds, T. A.; Hseu, T. H.; Wagnon, J. C.; Devon, T.; Tancrede, J.; McKennis, J. S.; Pettit, R. *J. Am. Chem. Soc.* **1974**, *96*, 7562. (b) Rigby, J. H.; Henshilwood, J. A. *J. Am. Chem. Soc.* **1991**, *113*, 5122. (c) Chaffee, K.; Huo, P.; Sheridan, J. B.; Barbieri, A.; Aistars, A.; Lalancette, R. A.; Ostrander, R. L.; Rheingold, A. L. *J. Am. Chem. Soc.* **1995**, *117*, 1900.
(34) Kroke, E.; Weidenbruch, M.; Saak, W.; Pohl, S.; Marsmann, H. *Organometallics* **1995**, *14*, 5695.
(35) Summerscales, O. T.; Fettinger, J. C.; Power, P. P. *J. Am. Chem. Soc.* **2011**, *133*, 11960.
(36) Özkar, S.; Kurz, H.; Neugebauer, D.; Kreiter, C. G. *J. Organomet. Chem.* **1978**, *160*, 115.
(37) Mach, K.; Antropiusová, H.; Petrusová, L.; Hanuš, V.; Tureček, F.; Sedmera, P. *Tetrahedron* **1984**, *40*, 3295.
(38) Jenner, G.; Papadopoulos, M. *J. Org. Chem.* **1986**, *51*, 585.
(39) (a) Hurni, K.; Baines, K. M. *Chem. Commun.* **2011**, *47*, 8382. (b) Dixon, C. R.; Baines, K. M. *Phosphorus, Sulfur Silicon Relat. Elem.* **1997**, *124*−*125*, 123. (c) Jung, Y.; Brynda, M.; Power, P. P.; Head-Gordon, M. *J. Am. Chem. Soc.* **2006**, *128*, 7185.
(40) Woodward, R. B.; Hoffmann, R. *Angew. Chem., Int. Ed. Engl.* **1969**, *8*, 781.
(41) (a) West, R. *Angew. Chem., Int. Ed. Engl.* **1987**, *26*, 1201. (b) West, R. *Angew. Chem.* **1987**, *99*, 1231.
(42) Smith, C. D. *J. Am. Chem. Soc.* **1966**, *88*, 4273.
(43) (a) Doering, W. v. E.; Hoffman, A. K. *J. Am. Chem. Soc.* **1954**, *76*, 6162. (b) Jefford, C. W.; Kabengele, N.; Kovacs, J.; Burger, U. *Helv. Chim. Acta* **1974**, *57*, 104. (c) Jefford, C. W.; Kabengele, nT.; Kovacs, J.; Burger, U. *Tetrahedron Lett.* **1974**, *15*, 257. (d) Jefford, C. W.; Mareda, J.; Gehret, J. C. E.; Kebengele, T.; Graham, W. D.; Burger, U. *J. Am. Chem. Soc.* **1976**, *98*, 2585. (e) Jefford, C. W.; Huy, P. T. *Tetrahedron Lett.* **1980**, *21*, 755. (f) Misslitz, U.; Jones, M. J.; de Meijere, A. *Tetrahedron Lett.* **1985**, *26*, 5403.
(44) (a) Barton, T. J.; Juvet, M. *Tetrahedron Lett.* **1975**, *16*, 3893. (b) Kroke, E.; Will, P.; Weidenbruch, M. Silylene and Disilene Additions to the Double Bonds of Alkenes, 1,3-Dienes, and Hetero-1,3-Dienes. In *Organosilicon Chemistry II: From Molecules to Materials*; Auner, N., Weis, J., Eds.; VCH: Weinheim, Germany, 1996; p 309. (c) Haaf, M.; Schmedake, T. A.; West, R. *Acc. Chem. Res.* **2000**, *33*, 704.
(45) (a) Schriewer, M.; Neumann, W. P. *J. Am. Chem. Soc.* **1983**, *105*, 897. (b) Huck, L. A.; Leigh, W. J. *Organometallics* **2009**, *28*, 6777.